Alterations in the Brain Lipidome of Alzheimer's Disease Donors with Rare TREM2 Risk Variants

Petroula Proitsi,[1,2#] Amera Ebshiana,[3] Asger Wretlind,[3] Jin Xu,[1,3] Angela Hodges[2*#] and Cristina Legido-Quigley[3,4*#]

***These authors contributed equally to this work:**

Angela Hodges & Cristina Legido-Quigley

[#]Co-corresponding authors:

Petroula Proitsi, Angela Hodges & Cristina Legido-Quigley

Author affiliations:

1. Centre for Preventive Neurology, Wolfson Institute of Population Health, Queen Mary University of London, London, EC1M 6BQ, UK
2. Maurice Wohl Clinical Neuroscience Institute, Institute of Psychiatry, Psychology and Neuroscience (IoPPN), King's College London, London, SE5 9RT, UK
3. Institute of Pharmaceutical Science, King's College London, London, UK
4. Steno Diabetes Center Copenhagen, Borgmester Ib Juuls Vej 83, 2730 Herlev, Denmark

Running title: Brain lipids, Alzheimer's and *TREM2*

Keywords: TREM2; Alzheimer's Disease; brain, lipids; lipidomics; Sphingolipids; phospholipids; genetics; network analysis

Abstract

TREM2 is a microglial receptor, sensitive to Phospholipids and Sphingomyelins, associated with neurodegeneration. Hypomorphic variants in the *TREM2* gene significantly increase the risk of developing AD.

The main aim of this study was to characterize networks of lipids in post-mortem brain from AD and control donors, and to identify key lipids that are associated with AD and impacted by dysfunctional TREM2.

We studied human post-mortem brain tissue from the hippocampus and the BA9 pre-association cortex from a total of 102 post-mortem brains. Specifically, brain tissue from the BA9 pre-association cortex was available for n=55 donors and brain tissue from the hippocampus was available for n=47 brain donors from three groups: AD donors with a non-synonymous risk DNA variant in *TREM2* (AD-TREM2^{var}), AD donors with no *TREM2*-associated variant (AD-TREM2^{wt}), and control donors. Mass Spectrometry was performed to obtain lipidomic signatures spanning 99 lipid species that included the following lipid classes: Ceramides, Sphingomyelins, Phosphatidic acids, Phopshatidyl-cholines, Phosphatidyl-ethalonamines, Phosphatidyl-glycerols, Phosphatidyl-inositols, Phosphatidyl-serines and Triglycerides. Weighted gene co-expression network analysis (WGCNA) was used to identify highly correlated lipid modules and 'hub' lipids. Linear mixed models and linear regression analyses, adjusted for age, biological sex, number of APOEε4 alleles and post-mortem delay were used to assess the association of modules and individual hub lipids with AD and *TREM2* status.

Four lipid modules were found to be relatively well-preserved between the two brain regions, and three of these modules were altered in AD donors and/or in AD donors with *TREM2* genetic variants. Levels of the BA9 "turquoise" module ("blue" hippocampus module), enriched in Sphingolipids and Phospholipids, were elevated in AD brain donors and in AD TREM2 carriers. The key lipid (hub) of the BA9 "turquoise"/ hippocampus "blue" module was a Phosphatidylserine (PS(32:1)), increased in both AD donors and TREM2 carriers (AD-TREM2^{wt} versus controls: beta=0.468, 95% CI 0.05 - 0.89, p= 3.02E-02; and AD-TREM2^{var} versus controls: beta=1.00, 95% CI 0.53 - 1.47, p= 5.57E-03), whereas the strongest association was observed with a Ceramide (Cer(d38:1)) (AD-TREM2^{wt} versus controls:

beta=0.663, 95% CI 0.17 - 1.16, p= 8.9E-03; and AD-TREM2^{var} versus controls: beta=1.31, 95% CI 0.78 - 1.84, p= 4.35E-06).

The consistent increase in TREM2 ligands such as Ceramides and Phosphatidyl-serines in the brains of AD donors, particularly in carriers of *TREM2* risk variants, could reflect the presence of AD-associated damage signals in the form of stressed/apoptotic cells and damaged myelin.

Introduction

Life expectancy has steadily increased in recent years, but with it brings greater prevalence of age-related conditions such as Alzheimer's disease (AD), the most common cause of dementia. Dementia numbers are predicted to grow from 46.8M to 131.5M by 2050[1] highlighting the urgent need for effective treatments. DNA variants linked to ~84 genes are consistently associated with AD risk, of which ~25% have highly enriched or specific expression in brain microglia (reviewed in[2]). Genes with immune or lipid function have been recognised for some time to be enriched in AD GWAS results[3]. One of these genes *TREM2*, codes for the Triggering receptor expressed on Myeloid Cells 2. Rare, but large-impact hypomorphic variants in *TREM2* significantly increase AD risk[4-7] and related conditions[8-12]. Rare recessive *TREM2* mutations can also cause Nasu-Hakola disease characterised by fragility fractures, brain white matter changes and dementia in early adulthood[13].

Most *TREM2* risk variants cluster in the extracellular Ig-like V-type domain impacting production (rs104894002, Q33X), expression or turnover of TREM2 at the cell surface (rs75932628, R47H)[14,15], α-secretase cleavage of the extracellular ectodomain (sTREM2 production) (rs2234255, H157Y)[15-17], shedding of sTREM2 (rs75932628, R47H)[18] and/or ligand binding (rs75932628, R47H; rs143332484, R62H; rs2234253/rs2234258/rs2234256, T96K/W191X/L211P; rs2234255, H157Y)[19-21].

TREM2 is a damage-response receptor expressed exclusively by myeloid cells including brain microglia[22]. It has a preference for binding anionic lipids, notably Phosphatidyl-serine (PS)[21,23-25] a membrane signal on apoptotic cells, notably neuronal synapses in AD[26]. Other lipids reported to activate TREM2 include Phosphatidyl-ethanol (PE), Phosphatidyl-choline (PC), Phospholipids, and Sphingolipids such as Ceramides (Cer) and Sphingomyelins (SM). Damaged oligodendrocyte myelin and stressed or apoptotic cells expose sphingolipids in AD[19-21,23,24,27-31]. APOE and other apolipoproteins and Aβ oligomers also appear to be ligands for TREM2[20,32-36].

TREM2-related pathologies include regional brain atrophy, myelin loss, swollen axons in white matter and changes the density and shape of microglia subsets[37,38]. TREM2 dysfunction prevents microglia from switching to a glycolytic state[39] resulting in deficits in Aβ, myelin debris, apoptotic neuron and *E.coli* phagocytosis[15,40-43]. Results from analysis of very rare *TREM2* risk cases is limited. Nevertheless, non-hydroxy fatty acids of sulfatide (C16-C18)

were found to be higher in Nasu-Hakola cortex compared to matched controls, while longer-chain (C24) fatty acids were lower[44]. Additionally, free fatty acids were increased[45] while cholesterol and Ceramides in white matter were reduced[46]. Microglia from a cuprizone demyelinating TREM2-deficient mouse model were found to still sense and take up myelin debris but failed to efflux myelin cholesterol, resulting in cellular cholesteryl ester (CE) accumulation[25]. In that same study, shorter fatty acid Ceramides were elevated indicative of inflammation. Together, TREM2 deficiency appears to lead to broad lipid dysregulation.

In AD cases with a *TREM2* risk variant, plaques are more diffuse and nearby microglia have reduced membrane ruffling, and shorter but more numerous filopodia when stimulated with ATP or M-CSF[47]. Loss of TREM2 impairs actin ring formation and podosomes in osteoclasts, essential for phagocytosis linked to bone resorption[48]. PIP2 to PIP3 conversion at the cell membrane is essential for 'sealing off' the membrane edges during motility, endocytosis, exocytosis and phagocytosis through the cytoskeletal system. TREM2 signalling links to this pathway through Syk, MAPK, PIP2-PI3K-PIP3 Rac1 and Cdc42involving lipid species[31,49].

Over-expression, activation or restoration of normal TREM2 function has largely beneficial outcomes in amyloidogenic mouse models[50-53] while knock-out or haploinsufficiency exacerbates amyloid-associated pathologies[54-58]. These benefits are likely linked to improved phagocytosis of amyloid and clearance of damaged neurons by phagocytosis. It is noteworthy that amyloid plaques contain various lipids (Sphingolipids such as Ceramides, Phospholipids, Lysophospholipids as well as Cholesterol and Triglycerides) which may themselves influence pathogenesis[59-61]. Ceramides are potent inflammatory signalling molecules associated with AD in circulation[62].

We hypothesize brain lipid dysregulation in AD reflects unresolved pathologies (damaged myelin, stressed/dying neurons and their knock-on impacts on lipid metabolism and membrane composition) exacerbated in people with a TREM2 risk variant where microglia fail to recognise and clear these pathologies effectively. Here, we sought to characterize networks or "modules" of highly connected lipids in post-mortem brain tissue from AD and control donors, and to identify key lipid "hubs," i.e., highly connected lipids likely to play central roles in the functioning and regulation of these networks, associated with AD and impacted by TREM2. Specifically, we used a network approach used traditionally for genomic data, Weighted Gene Correlation Network Analysis (WGCNA), in post-mortem brain from two areas, the Hippocampus (HC) and the BA9 pre-association cortex. We investigated whether these

networks and their "hubs" were altered in brain tissue from AD donors compared to control donors, and in brain tissue from AD carriers of rare *TREM2* risk variants (TREM2^{var}) compared to controls and AD donors with no TREM2 risk variants (TREM2^{wt}). Results from this study highlight lipid networks of highly correlated lipids and key "hubs" connected to AD pathology. It also provides insights into the role of lipids in TREM2-mediated activation of microglia in AD, which together highlight processes to target in future therapeutic strategies.

Materials and Methods

Study participants and samples

Informed consent for all brain donors was obtained according to the Declaration of Helsinki (1991) and protocols and procedures were approved by the relevant ethical committee and by each brain bank. Brain tissue was provided following project approval by the London Neurodegenerative Diseases Brain Bank (LNDBB). LNDBB subjects were approached in-life for written consent for brain banking, and all tissue donations were collected, stored and distributed following legal and ethical approval (Wales REC 3 favourable opinion 17 Sep 2013, REC number 08/MRE09/38+5; LBBND HTA license number 12293).

Pathological diagnosis was made according to established methods at the time of donation[63-67]. Where necessary for historical cases, retrospective diagnoses were made using current criteria. Post mortem human brain tissue, from the Hippocampus (HC) and BA9 pre-association cortex from n=60 brain donors were obtained for three groups: AD/TREM2^{var} (AD donors with a non-synonymous high AD risk DNA variant in TREM2), 20 AD/TREM2^{wt} (AD donors with AD-associated TREM2 variant) and 21 Control/TREM2^{wt} (tissue from age-matched donors absence of AD pathology or AD-associated TREM2 variant).

The TREM2^{var} group were selected from 19 donors: 9 donors identified by sequencing TREM2 Exon 2 in 631 AD and normal elderly control brain donors from the MRC London Neurodegenerative Diseases Brain Bank; 4 donors identified from a screen of 198 AD cases from The Netherlands Brain Bank (Royal Netherlands Academy of Arts and Sciences, Netherlands) and a further 6 donors described previously[4] from the Queen Square Brain Bank for Neurological Disorders. From these, 14 had a pathologically confirmed diagnosis of AD while 5 were pathologically normal at death, although one displayed symptoms of mild

cognitive impairment just prior to death and were subsequently assessed as Braak stage III at post-mortem. Consequently n=14 with AD were included in the AD/ TREM2^{var} group of which the majority were *TREM2* c.140G>A; p.R47H (rs75932628). One donor had a novel variant while the remaining variants have been described previously in AD cases (Table 1 and Table S1). In total, BA9 pre-association cortex was available for 55 donors while hippocampus (HC) was available for 47 donors (Table 1 and Table S1).

Sample Preparation

Samples were randomized and lipids extracted based on an in-vial dual extraction (IVDE) protocol[68]. Briefly, 10µl of water was added to 50µl of the homogenate. Vials were then vortexed for 5 minutes, after which 250µl of methyl-tertiary butyl ether (MTBE) containing Tripentadecanoin (10µg/ml) and Heptadecanoic acid (10µg/ml) was added, and samples were again vortexed at room temperature for 60 minutes. Following the addition of a further 40µl of water containing 0.15mM ammonium, samples were centrifuged at 2500×g for 30 minutes at 4°C. This resulted in clear separation of an upper MTBE and lower aqueous phase.

Data Acquisition

LC-MS Lipidomics analysis of the upper MTBE layer in positive mode was performed on a Waters Acquity ultra performance liquid chromatogram (UPLC) system coupled to a Waters Premier quadrupole time-of-flight (Q-Tof) mass spectrometer (Waters, Milford, MA, USA). Briefly, 5 µl of sample extract was injected onto an Agilent Poroshell 120 EC-C8 column (150mm × 2.1mm, 2.7µm). The gradient started at 80% mobile phase B increasing linearly to 96% B in 23 minutes and was held until 45 minutes then the gradient was increased to 100% by 46 minutes until 49 minutes. Initial conditions were restored in 2 minutes ahead of 7 minutes of column re-equilibration. Data were collected in the centroid mode over the mass range m/z 50–1000 with an acquisition time of 0.1 secondsper scan. Samples were analysed in a randomized order along with pooled brain samples (Quality control samples) after every eight injections.

Data Pre-processing and Lipid Identification

All data was collected by Waters Xevo QTOF which used a MSe technique. Two collision energies were applied enabling data collection at two levels. The first level obtained data using 5 V of collision energy, the second level obtained data at a higher collision energy of

50 V. This can assist in structural elucidation and to simultaneously collect accurate mass of parent ion and fragmentation data. Following LC-MS analysis of samples, the MS raw data were transformed into mzXML format using msConvert (ProteoWizard). XCMS software package in R was then used to analyse the converted mzXML data files, which underwent preprocessing steps of peak picking and alignment processed, using a 'centwave' method which enables the deconvolution of closely eluting or slightly overlapping peaks. Data was normalised to total peak area, imputed and inverse variance transformed.

A total of 99 lipids were identified in the brain samples following our previous established protocol[69]. Identification was based on fragmentation patterns and comparison with lipid features from our in-house lipid library containing pure standards. Lipid species were examined in positive ion mode and the product ions of the$[M+H]^+$ precursor was used to determine their acyl composition. As an example, the fragment ion 184.03Da corresponds to phosphocholine head group. Twenty-six Sphingolipids (16 Sphingomyelins and 10 Ceramides) were identified with a parent molecular ion in the form$[M-H2O+H]^+$ and the fragment ion 264.26Da which corresponds to a Sphingosine base chain. We named the fatty acid chains as very long (VLCH), longer (LCH) or shorter (SCH), but these names are only for reference in this manuscript, as there isn't a single universal standard specifically for lipid naming based on chain length.

Statistical Analysis

Data Quality Control

Lipid features missing in ≥20% of donors, and donors with ≥20% missing features were excluded from further analyses. For the remaining data, missing data points (n=4) were imputed using k-nearest neighbours (knn, k=10) ("impute") and the dataset was subsequently inverse-normal-transformed.

Preliminary associations between lipids, brain regions and covariables

In preliminary analyses, we investigated the association of each lipid with sex, age (at death), number of APOEε4 alleles and post-mortem delay, combining the two brain regions (Supplementary Table 1). Linear model analysis was performed with lipids as outcomes using generalized least squares ('gls' function in nlme R package[70]), which allows for a fully unstructured residual variance-covariance matrix. Analyses were initially performed

separately for each covariable, adjusting for post-mortem delay with sex, age (at death), number of APOEε4 alleles as predictors. An interaction term between brain region and each predictor, was included in each model to investigate possible brain region-specific associations. In the presence of an interaction, linear regression analyses were repeated, stratifying for each brain region. To correct for multiple testing and the high correlation between some lipids (Supplementary Figure 1), we set a metabolome-wide statistical significance threshold of $p < 0.001$; the $p < 0.05$ significance level was divided by the number of principal components (n=45) that explained over 95% of variation in the lipidomic data.

Weighted Gene[Lipid] Co-expression Analysis

Network construction

To define lipid networks within the BA9 pre-association cortex and Hippocampus, we applied WGCNA to the lipid data for each brain region. Lipids were first adjusted for sex, age (at death) and post-mortem delay, separately in each region, and the standardized residuals were used for subsequent analyses. Next, the standardized connectivity ($Z.k$) for each sample was computed to identify outliers ($Z>|4|$). A pairwise correlation matrix using biweight midcorrelations between all lipids was then derived. From this, a weighted, signed adjacency matrix was constructed by raising correlations to a soft thresholding power of 12 for both modules, chosen to meet a scale-free topology threshold of ≥0.8, while maximizing mean connectivity.

Subsequently, the adjacency matrix was transformed into a topological overlap matrix (TOM), representing the network connectivity of lipids. Lipids were then hierarchically clustered into a dendrogram using an average linkage method based on their dissimilarity (1−TOM), and the dendrogram was cut using a dynamic hybrid tree cutting algorithm parameters—minModuleSize = 12 (to allow for smaller modules to be constructed), and mergeHeight = 0.25 (default)).

The resulting modules or groups of co-expressed lipids were used to calculate module eigengenes (MEs; or the 1st principal component of the module) for all modules. The ‘grey’ module comprised lipids that were not assigned to any particular module and was therefore dropped from further analyses.

Lipids that are highly connected to their module (termed "hub" lipids) are likely to be functionally important. To identify hubs lipids in each module, the associations between lipids and their assigned module (module membership; kME) were calculated using correlations between lipids and module eigenvalues. Lipids with a kME > 0.70 in each brain region were defined as hubs.

Module preservation between BA9 and Hippocampus

To investigate whether modules between the two brain regions showed similar coexpression/connectivity and were thus preserved, we utilized the WGCNA "modulePreservation" function. Module preservation and robustness was summarised by reporting Z summary scores, a composite measure of 4 statistics related to density and 3 statistics related to connectivity. The module preservation analysis was applied twice assigning one as the reference dataset and the other as the test dataset. Summary values between 2 and 10 are considered to be moderately preserved (reproducible), while those below 2 are considered not preserved, and those above 10 are considered strongly preserved[71].

Associations between lipid modules, AD and TREM2 in each brain region

Following WGCNA analyses, we sought to investigate the association between lipid modules in each brain region and 1) Post-mortem AD diagnosis (i.e. combining AD/TREM2^{var} and AD/TREM2^{WT}) *vs* Control/TREM2^{WT} donors. To probe whether any associations of brain lipid modules with AD diagnosis were driven by genetic variation at the TREM2 locus we then compared brain lipid module levels in 2) AD/TREM2^{WT} brain donors *vs* Control/TREM2^{WT} donors, 3) AD/TREM2^{var} *vs* Control/TREM2^{WT} donors, and finally,4) TREM2^{var} *vs* TREM2^{WT} in AD donors only (i.e. AD/TREM2^{var} *vs* AD/TREM2^{WT}). Analyses were performed for each brain region separately by regressing the residualised lipid modules generated through WGCNA against the outcomes using linear regression analyses and further adjusting for the number of APOEε4 alleles. To investigate the association of APOEε4 with lipid modules, separate regression analyses between each module and the number of APOEε4 alleles were additionally fitted. For all module analyses, a Bonferroni-corrected significance threshold was set at $p < 0.05/$ Number of modules for each brain region(4) = 0.0125.

Associations between hub lipids, AD and TREM2

We finally investigated the associations with hub lipids (kME>0.70) in modules associated with AD and/or TREM2 in either brain region by performing a linear model analysis using generalized least squares, as described above, and by adjusting for the number of APOEε4 alleles. To further identify brain region-specific associations, an interaction between diagnosis and variant status and brain region was included in each GLS model. To avoid multiple testing issues, an interaction was considered between brain region and AD vs Controls, and between brain region and AD/TREM2^{WT} vs AD/TREM2^{var}, as these would capture brain region AD-specific or TREM2-specific effects. In the presence of an interaction ($p<0.05$), linear regression analyses were repeated, stratifying for each brain region. For all hub analyses, a Bonferroni-corrected significance threshold was set at $p< 0.05/ 31$ (Number of hubs) = 0.0016.

Analyses were conducted in RStudio (R version 3.4.2).

Results

Donor and sample characteristics

The demographic characteristics of the cohort for each brain region are described in Table 1. Overall, BA9 pre-association cortex tissue was available for 55 donors while hippocampus tissue was available for 47 donors. Although AD donors were generally older, and more likely to be female, there was no statistical difference between age at death, post-mortem delay. The ratio of men to women was similar across groups (p=>0.05) (Table 1). Of the 99 annotated lipids 10 were Ceramides (CER), 16 were Sphingomyelins (SM), 6 were Phosphatidic acids (PA), 22 were Phopshatidy-lcholines (PC, including 4 Lyso-phospholipids), 2 were Phosphatidyl-glycerols (PG), 6 were Phosphatidyl-inositols (PI), 13 were Phosphatidyl-serines (PS), 12 were Phosphatidyl-ethanolamines and 12 were Triglycerides (TG). Overall, PS levels were higher compared to other lipids (Supplementary Figure 2).

Associations of lipids with age at death, sex, APOEε4 genotype and post-mortem delay

Most lipids had different levels in BA9 compared to hippocampus. After controlling for multiple testing, 55 out of 99 lipids differed between the two brain regions, 32 of which were lower in the hippocampus and 23 higher in the hippocampus compared to BA9 (Supplementary Table 1).

Following correction for multiple testing, only one lipid, Phosphatidyl-choline (PC(38:2)), showed an association with the number of APOEε4 alleles (beta=-0.49, 95% CI = -0.78 – -0.21, p=0.0009). No lipids were associated with sex, age at death or post-mortem delay. Overall, the association of lipids with the covariates were consistent between the two brain regions, in terms of direction of effects, with no interactions present after multiple testing correction (Supplementary Table 1).

Network analyses

WGCNA analysis identified four modules in each brain region, comprising 16–22 lipids in the BA9 cortex and 14-26 lipids in the Hippocampus. A grey module (lipids not assigned to one of the four modules) included the remaining 22 and 17 lipids, respectively.

The four modules identified in BA9 were the turquoise module, comprising mainly of Longer Chain Ceramides and SMs, and Medium Chain Phosphatidyl-choline (PC) lipid species; the yellow module comprising mainly Very Long Chain Phospholipids; the brown module comprising Very Long Chain SMs and Phospholipids, and the blue module comprising mainly Triglycerides (TGs).

In the Hippocampus, the blue module (corresponding to the BA9 turquoise module) comprised mainly Longer Chain Ceramides and SMs, and medium chain PC lipid species; the yellow module (equivalent to the BA9 yellow module) comprising mainly Very Long Chain Phospholipids; the turquoise module (corresponding to the BA9 brown and yellow modules) comprising mainly Very Long Chain Phospholipids and Sphingolipids; and the brown module (corresponding to the BA9 blue module) comprising mainly TGs. Module preservation analyses indicated that all four lipid modules showed medium-to-high preservation and reproducibility between the two brain regions (Supplementary Figure 3).

Module-level regression analyses

BA9

In linear regression analyses, AD donors had higher turquoise module levels and lower yellow module levels compared to control donors after adjustment for multiple testing (beta= 1.003, 95% CI =0.42 -1.59, p=0.001 and beta= -0.821, 95% CI =-1.44 - -0.20, p =0.011, respectively) (Figure 2 and Supplementary Table 2). We next sought to explore whether any associations in lipid module levels observed between AD and control brains were driven by TREM2 risk variants, by separating AD/ $TREM2^{WT}$ and AD/$TREM2^{var}$ donors. For the turquoise module, we observed additive AD and TREM2 effects, whereby levels of lipids in the turquoise module were increased on average by 0.76 SD in AD/ $TREM2^{WT}$ donors compared to controls (95% CI = 0.13 – 1.37, p =0.019) and by 1.35 in AD/ $TREM2^{var}$ donors compared to controls (95% CI = 0.69 – 2.01, p = $1.467* 10^{-4}$), although only the association between AD/ $TREM2^{var}$ donors and controls survived multiple testing correction. Comparing BA9 turquoise module levels between AD/ $TREM2^{WT}$ donors and AD/ $TREM2^{var}$ donors highlighted a modest increase in TREM2 carriers (beta=0.601, 95% CI= 0.008 – 1.19, p =0.047). On the other hand, the decrease in yellow module levels in AD/ $TREM2^{WT}$ donors relative to controls was similar to that observed in AD/ $TREM2^{var}$ donors compared to controls (beta=-0.834, 95% CI -1.52 to -0.145, p =0.019 and beta=-0.03, 95% CI -1.54 to -0.07 p =0.032 respectively), highlighting no additional effect of TREM2 on lipid levels in the yellow module (TREM2-independent associations). None of these associations were significant after correction for multiple testing (Figure 2 and Supplementary Table 2).

We also observed higher brown module lipid levels and lower blue module levels in AD/ $TREM2^{WT}$ carriers vs AD/ $TREM2^{var}$ (AD-independent associations), although only the association with the brown module survived multiple testing (beta=0.958, 95% CI= 0.29 – 1.64, p =0.006). Finally, we observed a nominal positive association between the turquoise module and the number of APOEε4 alleles testing (beta=0.443, 95% CI= 0.07 – 0.81, p =0.020).

Hippocampus

Linear regression analyses revealed that the direction of effect of the observed associations in the Hippocampus was similar to those observed in BA9, particularly for the Hippocampus blue module (corresponding to the BA9 turquoise module). However, the strength of the

associations in the hippocampus was weaker to that in BA9 with no nominal associations observed (Figure 2 and Supplementary Table 2).

Association of hub lipids with AD and TREM2

We next sought to identify associations between hub lipids that were highly connected (kME>0.70) in modules associated with AD and/or TREM2 after correction for multiple testing i.e. the BA9 turquoise, brown and yellow modules. The candidate 31 hubs included 12 lipids from the BA9 turquoise module, 12 lipids from the BA9 yellow module and 7 lipids from the BA9 brown module. The top hub for the BA9 turquoise module was Phosphatidyl-serine (PS) (PS(32:1)), followed by longer chain Ceramides and SM, and Phosphatidyl-ethalonamines; the key hub for the BA9 yellow module was Phosphatic Acid (PA 36:1) followed by other phospholipids; and the key hub for the BA9 brown module was SM (SM d44:2), followed by other SMs. Since all the modules showed medium-high preservation between the two brain regions, joint brain-area analyses were performed for each lipid using generalised least squares (GLS) and setting a Bonferroni-corrected significance threshold at $p< 0.05/ 31= 0.0016$.

Overall, ten hub lipids were found to be associated with AD and/or TREM2 status after multiple testing correction (Figure 3, Supplementary Table 3). All ten lipids were in the BA9 turquoise module (HC blue module) that consisted of medium chain Phospholipids and longer chain Sphingolipids.

Notably, six of the lipids were increased in AD compared to controls after adjustment for multiple testing. The strongest relationship was with Ceramide (Cer(d38:1); beta=0.929, 95% CI 0.46 - 1.40, p= 1.68E-04) (Figures 3 and 4), with the remaining associations with three Ceramides, one Sphingomyelin (SM(d36:1)) and with the BA9 turquoise and HC blue modules key hub Phopsphatidyl-serine (PS(32:1)) (beta=0.677, 95% CI 0.28- 1.08, p= 1.14E-03).

We then sought to explore whether any associations between the six hub lipids and AD were driven by TREM2 risk genotypes. Similarly to module level analyses, GLS analyses for both brain regions highlighted an increase in all BA9 turquoise / HC blue lipid levels ranging from ~0.47 SD to ~0.76 SD between AD/ $TREM2^{WT}$ donors and controls, and an increase in lipid

levels ranging from ~0.80 SD to ~1.31 SD between AD/ TREM2^{var} donors and controls, highlighting on average an increase of ~0.5 SD in lipids levels between AD/ TREM2^{WT} and AD/ TREM2^{var}. Although the associations between AD/ TREM2^{WT} and controls were nominal ($p<0.05$), all six associations between AD/ TREM2^{var} and controls were significant after correction for multiple testing (Figure 3 and Supplementary Table 3). The strongest association was again with Cer(d38:1)) (beta=1.310, 95% CI 0.78 – 1.84, p= 4.35E-06). We also observed four additional lipid hubs, all belonging to the BA9 turquoise / HC blue modules, that were increased in AD/ TREM2^{var} vs controls after correction for multiple testing, and which had shown only nominal associations with AD status (Figure 3, Supplementary Table 3). These results highlight additive AD and TREM2 effects for most lipids in the BA9 turquoise and HC blue modules. Finally, we observed some associations with hub lipids in other modules suggesting TREM2-independent and AD-independent effects and reflecting the results observed at module level. None of these associations remained significant after adjustment for multiple testing (Supplementary Table 3).

Brain region specific association of lipids with AD and TREM2 variants

Overall, we found associations between brain lipids and end-stage AD with or without a TREM2 mutation to be consistent between the two brain regions, particularly for the BA9 turquoise /hippocampus blue modules, with overall stronger effects observed for BA9.

There was weak evidence for brain-region-specific associations between TREM2 and lipids belonging to the BA9 yellow module, where hub Phospholipids were higher in AD donors compared to controls, with no further increase in TREM2 carriers (TREM2-independent associations) (interaction Pvalue <0.5) (Supplementary Table 3). We also observed that the levels of hub lipids belonging to the BA9 brown module, particularly SMs, were increased in AD/ TREM2^{var} compared to AD/ TREM2^{WT} (AD-independent associations) (interaction Pvalue <0.5), although these relationships did not survive multiple testing correction (Supplementary Table 3).

Discussion

Here, we characterized lipid networks in 102 post-mortem brain samples from 55 AD and control donors, identifying key lipids associated with AD and impacted by dysfunctional TREM2. TREM2 is an established lipid receptor uniquely expressed by microglia in the brain. It is also a risk gene for AD[19-21,23,27-31]. Four modules consisting of highly correlated lipids were well-preserved between the BA9 pre-association cortex, and hippocampus. Lipid levels in the BA9 "turquoise" module (hippocampus "blue" module) were significantly elevated in post-mortem tissue form AD donors compared to controls. Levels were even higher in AD donors who additionally had a loss-of-function TREM2 AD risk variant. The BA9 "turquoise"/hippocampus "blue" module was enriched in longer chain Sphingolipids (Ceramides and Sphingomyelins), and Phospholipids including Phosphatidyl-serines. Overall, the strongest associations were observed with Ceramides, whereas the key hub lipid i.e. lipid with the highest number of connections to other lipids in this module, was Phosphatidyl-serine PS(32:1) in BA9 and hippocampus. These findings further implicate TREM2 in lipid regulation.

Phosphatidyl-serine a major component of cell membranes, is normally confined to the inner cytoplasmic leaflet by transporter proteins flippase and floppase. However, when these enzymes are inactivated during cell death, it becomes exposed on the outer plasma membrane [72] becoming a phagocytic signal for macrophages including microglia[73,74]. Local exposure of Phosphatidyl-serine on neurons can impact spine engulfment and thus neural activity[26]. Phosphatidyl-serine can also impact the structure and function of membrane nanodomains, including cholesterol linked functions[75]. Phosphatidyl-serine is an established ligand for the TREM2 receptor[21,23-25]. Our data shows that levels of Phosphatidyl-serine were even higher in *TREM2* AD risk variant carriers suggesting a failure by microglia to recognise and clear dysfunctional neurons. Senescent AD microglia are considered poor at degrading aggregate pathologies, leading to aggregate spreading and seeding [76-79]. Nevertheless, they appear very capable of phagocytosing soma, nucleus and apical dendrites of neuronal corpses and together with astrocytes can fully degrade neurons[80]. In the course of clearing or partially clearing neuronal corpses in AD brain, insoluble extracellular neurofibrillary "ghost tangles" are left where neurons once resided [81]. This suggests cell membranes containing Phosphatidyl-serine can be cleared in AD, although whether microglia partially or fully clear neurons in AD in those with a TREM2 risk variant has not been investigated. In microglia where TREM2 function is compromised, they fail to switch from homeostatic OXPHOS to activated glycolysis[39] necessary to drive phagocytic function[23,82] including of myelin

debris[24]. It would be interesting to evaluate the number of "ghost tangles" in TREM2 cases and establish whether membrane remnants remain at these sites to better understand the contribution of TREM2 to neuronal clearance by microglia. A failure to remove apoptotic neurons in AD could lead to the persistence of damaging inflammatory signals from neurons such as HMGB1, DNA and IL-1α which in turn would exacerbate AD pathologies further[83-86]. It will also be important to evaluate the function of other microglia Phosphatidyl-serine receptors in the absence of TREM2 function. MERTK & Axl, integrin (ITGAV, ITGB3, ITGB5), HAVCR1 & TIMD4, ADGRB1, STAB1 (bridged by C1q), CD300f and LRP1 (bridged by Crt, C1q) are all highly or uniquely expressed by microglia[87] and may become preferential Phosphatidyl-serine receptors in the absence of TREM2, altering the function of microglia in AD.

Phosphatidyl-serine can exist with differing acyl length and saturation[88]. PS(32:1) was readily detectable in the two brain areas we investigated and showed the strongest association with AD and TREM2, although PS(34:2) was the most abundant in our samples. There were 13 PS molecules detected in our study, four of which belonged to the BA9 "turquoise" module / hippocampus "blue" module, where levels were increased in AD and TREM2. It is unknown if there is a preference for different PS species by TREM2 and other PS receptors or why certain PS species are selectively elevated in AD. Phosphatidyl-serine is not only present in neurons, but is also highly abundant in myelin[89] and other cell types (astrocytes and microglia)[90], and these could also be a source of the elevated levels we observed in AD and in those with dysfunctional TREM2. Myelin levels could be particularly relevant in light of the raised Ceramide levels we also observed in AD, particularly in those with a TREM2 risk variant and our finding that TREM2 is central to the co-ordination of oligodendrocyte and microglia genes in AD[91].

The strongest association with AD and TREM2 dysfunction in our samples was with longer chain Ceramides. These lipids were important hubs within the BA9 "turquoise" and hippocampus "blue" module, with their kME being slightly lower than that of Phosphatidyl-serines. Ceramides (galactosylceramide and sulfatide species) are synthesised predominantly by oligodendrocytes in the brain where they are the dominant lipid component of myelin[89,90,92]. Ceramide species accumulate in AD brains[93] and leukodystrophies when dysfunctional enzymes required for their metabolism become dysfunctional. This leads to accumulation of intermediate lipid species, notably in microglia lysosomes[89,94]. Ceramides

are metabolised to Sphingomyelin and vice versa, hence they can be a breakdown product of Sphingomyelin metabolism[93]. This perhaps explains why Sphingomyelin and Ceramide species were highly correlated and both appeared in the same modules in our study. Together these results, suggest TREM2 mediated microglia function is linked to oligodendrocyte function in AD.

Much effort has consolidated our knowledge of lipid intermediates and the enzymes responsible for their biosynthesis. Acyl chain length and saturation can impact lipid function and intermediates reflect sequential biosynthesis via *de novo* or salvage β-oxidation pathways. Typically, fatty acid chains are categorised as short- (<C5 carbons), medium- (C8-C13 carbons), longer- (C14-C20 carbons) and very long (>C20 carbons), although these categories vary by lipid group[95,96] although there isn't an agreed single universal standard for lipid naming based on chain length. In our study, it was longer chain and not very long chain Ceramides which had increased levels in AD brain and in those with a TREM2 risk variant (notably Cer (d38.1)). Ceramides, play important roles in membrane integrity, and can had proinflammatory and apoptotic function. We and others have previously found longer chain Ceramides and SMs to be elevated in the plasma of AD/dementia patients and are associated with hippocampal atrophy[62,96-98]. Consistent with our findings, others have also reported elevated levels in AD brain[99,100]. A recent study has further reported that Ceramides mediate the effect of known AD genetic factors such as ABC7 in AD[101]. Ceramide species like the ones reported here have been also implicated in cardiometabolic and cerebrovascular diseases and we have further demonstrated associations with 6-year cardiovascular risk and all-cause mortality in a Type-1-Diabetes cohort[102]. As both Ceramides and SMs increase the risk of cardiovascular disease and insulin resistance it has been also suggested that increased cardiometabolic risk could be mediating the association of ceramides with dementia risk[96]. Finally, higher levels of Ceramides and SMs have been observed in a cuprizone model of myelin damage in mice in which TREM2 is absent[25]. In fact, sulfatides, which are synthesized from galactosylceramides, which in turn are derived from ceramides, are strong TREM2 activators[103]. We were unable to distinguish sulfatide species in our anlaysis.

In Nau-Hakola disease where there is complete loss of TREM2 function or its adapter DAP12, lysosomal function in microglia is impaired suggesting the possibility that the increased lipids we observed may be accumulating in microglia thus impacting there response to AD damage[104]. It will be interesting to establish if microglia from TREM2 AD patients

accumulate lipids[105], as was recently shown in AD patients carrying APOEε4[106]. Amyloid deposits also contain lipids including Ceramides[107] and this could be an additional source of the elevated Ceramides we measured. Overall, our results suggest a failure by microglia to recognise damage lipid signals and successfully mobilise to clear damaged myelin and cells in AD leading to accumulation of specific lipids.

Ceramides can be potent bioactive molecules. High levels of ceramide can cause a myriad of changes culminating in increased damaging reactive oxygen species, through blockade of the respiratory chain, mitophagy and activation of apoptotic factors linked to axonal degeneration and cell death[93,108,109]. Furthermore, altered membrane lipid composition, particularly galactoceramides, can impact APP processing and amyloidogenic Aβ production[108,110] and this along with increased TNF-α can impact enzymes that metabolise lipids including those required for Sphingomyelin to Ceramide metabolism, as well as factors linked to apoptosis of oligodendrocytes[111-113]. In microglia without fully functioning TREM2, a failure to recognise and resolve lipid signals adequately would exacerbate a cycle of damage.

We also found weak evidence for brain region-specific lipid changes. For example, very long chain SMs and Phospholipids in the BA9 brown module were increased in AD/TREM2^{var} compared to AD/TREM2^{WT} donors (AD-independent associations). Hubs within this module also showed nominal associations with TREM2, but only inBA9. Similarly, the BA9 yellow module, enriched in very long chain Phospholipids, was decreased in AD compared to control donors, with no further decrease observed in TREM2 carriers (TREM2-indenepdent association). Levels of two hub Phospholipids were increased in AD donors compared to controls in BA9 only, after adjustment for multiple testing (Supplementary Table 3). These findings warrant further investigation.

Finally, we found that Phosphatidyl-choline, PC(38:2) levels were lower in APOEε4 carriers and also in BA9 in AD donors, particularly those with a TREM2 risk variant (Supplementary Table 3). PC(38:2) showed borderline association with the BA9 yellow module (kME=0.694) and was a hub for the equivalent Hippocampus yellow module (kME=0.920). The relationship therefore between TREM2, APOE and PC(38:2) warrants further investigation. Phosphatidyl-cholines are primarily found in cell membranes including the monolayer encapsulating lipid droplets, a reservoir of neutral lipids and cholesterol esters that swell in AD microglia, particularly in the absence of TREM2 and in high risk APOEε4 carriers[106,114-

[117]. Their role extends beyond structural integrity, as they are an essential component of lipoproteins (VLDL/LDL/HDL) that facilitate transport of triacylglycerols/cholesterol to/from cells, a tightly regulated process, with APOE-containing LDL- and HDL-cholesterol particularly implicated in AD[118-120]. The decrease in brain Phosphatidyl-choline species in AD compared to control donors reflects reports by us and others in plasma [62,121-123]. Additionally, Phosphatidyl-choline species like the ones reported here have been positively associated with hippocampal brain volume and negatively with disease progression[62] , as well as with CSF Aβ1–42[124].

Although dysregulation of Sphingolipids and Glycerophospholipids in blood and brain has been previously reported by us and others[62,121-124], this is one of the first studies to comprehensively investigate changes in brain lipid levels in AD donors carrying rare TREM2 risk variants and the first to use two AD-affected brain regions. Others have investigated impacts of TREM2 on brain gene expression[91] and metabolites[125] with findings implicating microglia, oligodendrocyte and endothelial genes, notably those involved in complement and Fcγ receptor function, microglia-associated ribosomal genes and oligodendrocyte genes, particularly proteosomal subunits and amino acid and sphingolipid metabolism and vitamin pathways, respectively. Recently Novotny *et al.*,[125] compared metabolite levels in donated brain tissue from sporadic AD, familial AD and AD/TREM donors compared to control donors. They reported reduced levels of beta-citrylglutamate in AD and AD/TREM2 brains compared to controls, possibly related to lower energy metabolism, as well as reduced *α*-tocopherol and CDP-ethanolamine in AD/TREM2 brains compared to controls brains, and reduced ergothionine and N-acetylputrescine levels in AD compared to control brains. Future analyses should investigate associations between the lipids we identified, gene expression and protein levels to better understand the important molecular processes.

Our study has some limitations. The sample size was modest, particularly for the AD/TREM2^{var} group. However, the majority of donors had brain tissue from both areas for which findings were consistent. Our analyses are also limited to end-stage disease changes. The use of bulk tissue may obscure cell-type-specific lipid alterations. Future studies should focus on analyzing lipidomics for TREM2 carriers in larger cohorts investigate cell type changes and expand analyses to blood and CSF. It is also important to examine lipid changes in brains from ethnically diverse donors to generalize findings.

Overall, our results are consistent with TREM2 dysfunction interfering with the recognition and clearance of unhealthy neuronal cells, damaged myelin and lipid-containing amyloid. These findings could have great translational potential as they highlight processes to target in future therapeutic strategies.

Data availability statement

Data is available upon reasonable request from the corresponding authorsfs in collaboration with the authors.

Funding

Petroula Proitsi is funded by an Alzheimer's Research UK Senior Research Fellowship. The London Neurodegenerative Diseases Brain Bank is supported by the MRC and Brains for Dementia Research. Cristina Legido-Quigley and Agsger Wretlind thank LunbeckFonden R344-2020-989.

Competing interests

The authors report no competing interests.

References

1. Prince M, Wimo A, Guerchet M, Ali G-C, Wu Y-T, Prina M. *World Alzheimer Report 2015: The Global Impact of Dementia Prof Martin Prince, Prof Anders Wimo, Dr Maëlenn Guerchet, Miss Gemma-Claire Ali, Dr Yu-Tzu Wu and Dr Matthew Prina*. 2015. 2015.
2. Hodges AK, Piers TM, Collier D, Cousins O, Pocock JM. Pathways linking Alzheimer's disease risk genes expressed highly in microglia. *Neuroimmunology and Neuroinflammation*. 2021;8:[Online First]. doi:10.20517/2347-8659.2020.60
3. Jones L, Holmans PA, Hamshere ML, et al. Genetic Evidence Implicates the Immune System and Cholesterol Metabolism in the Aetiology of Alzheimer's Disease. *PLoS ONE*. 2010;5(11)NOT IN FILE.
4. Guerreiro R, Wojtas A, Bras J, Carrasquillo M, Rogaeva E, Majounie E. TREM2 variants in Alzheimer's disease. *N Engl J Med*. 2013;368:117 - 127.
5. Jonsson T, Stefansson H, Ph.D. SS, et al. Variant of TREM2 Associated with the Risk of Alzheimer's Disease. *New England Journal of Medicine*. 2013;368(0):107-116. doi:doi:10.1056/NEJMoa1211103

6. Jin S, Benitez B, Karch C, Cooper B, Skorupa T, Carrell D. Coding variants in TREM2 increase risk for Alzheimer's disease. *Hum Mol Genet*. 2014;23:5838 - 5846.
7. Ridge PG, Hoyt KB, Boehme K, et al. Assessment of the genetic variance of late-onset Alzheimer's disease. Article. *Neurobiol Aging*. May 2016;41:8. 200.e13. doi:10.1016/j.neurobiolaging.2016.02.024
8. Guerreiro RJ, Lohmann E, Bras JM, et al. Using Exome Sequencing to Reveal Mutations in TREM2 Presenting as a Frontotemporal Dementia-like Syndrome Without Bone Involvement. *Jama Neurology*. Jan 2013;70(1):78-84. doi:10.1001/jamaneurol.2013.579
9. Kleinberger G, Brendel M, Mracsko E, et al. The FTD-like syndrome causing TREM2 T66M mutation impairs microglia function, brain perfusion, and glucose metabolism. *Embo j*. Jul 3 2017;36(13):1837-1853. doi:10.15252/embj.201796516
10. Rayaprolu S, Mullen B, Baker M, Lynch T, Finger E, Seeley W. TREM2 in neurodegeneration: evidence for association of the p.R47H variant with frontotemporal dementia and Parkinson's disease. *Mol Neurodegener*. 2013;8:19.
11. Liu G, Liu Y, Jiang Q, et al. Convergent Genetic and Expression Datasets Highlight TREM2 in Parkinson's Disease Susceptibility. *Mol Neurobiol*. 2015/09/14 2015:1-8. doi:10.1007/s12035-015-9416-7
12. Zhou SL, Tan CC, Hou XH, Cao XP, Tan L, Yu JT. TREM2 Variants and Neurodegenerative Diseases: A Systematic Review and Meta-Analysis. *J Alzheimers Dis*. 2019;68(3):1171-1184. doi:10.3233/jad-181038
13. Madry H, Prudlo J, Grgic A, Freyschmidt J. Nasu-Hakola disease (PLOSL) - Report of five cases and review of the literature. *Clinical Orthopaedics and Related Research*. 2007;(454):262-269. NOT IN FILE.
14. Park JS, Ji IJ, Kim DH, An HJ, Yoon SY. The Alzheimer's Disease-Associated R47HVariant of TREM2 Has an Altered Glycosylation Pattern and Protein Stability. *Frontiers in Neuroscience*. Jan 2017;10618. doi:10.3389/fnins.2016.00618
15. Kleinberger G, Yamanishi Y, Suárez-Calvet M, Czirr E, Lohmann E, Cuyvers E. TREM2 mutations implicated in neurodegeneration impair cell surface transport and phagocytosis. *Sci Transl Med*. 2014;6doi:10.1126/scitranslmed.3009093
16. Thornton P, Sevalle J, Deery MJ, et al. TREM2 shedding by cleavage at the H157-S158 bond is accelerated for the Alzheimer's disease-associated H157Y variant. *Embo Molecular Medicine*. 2017;doi:10.15252/emmm.201707673
17. Jiang T, Hou JK, Gao Q, et al. TREM2 p.H157Y Variant and the Risk of Alzheimer's Disease: A Meta-Analysis Involving 14,510 Subjects. *Current Neurovascular Research*. 2016;13(4):318-320. doi:10.2174/1567202613666160808095530
18. Hall-Roberts H, Agarwal D, Obst J, et al. TREM2 Alzheimer's variant R47H causes similar transcriptional dysregulation to knockout, yet only subtle functional phenotypes in human iPSC-derived macrophages. *Alzheimer's Research & Therapy*. 2020/11/16 2020;12(1):151. doi:10.1186/s13195-020-00709-z
19. Kober DL, Alexander-Brett JM, Karch CM, et al. Neurodegenerative disease mutations in TREM2 reveal a functional surface and distinct loss-of-function mechanisms. JOUR. *eLife*. 2016/12/20 2016;5:e20391. doi:10.7554/eLife.20391
20. Song W, Hooli B, Mullin K, et al. Alzheimer's disease-associated TREM2 variants exhibit either decreased or increased ligand-dependent activation. *Alzheimers & Dementia*. Apr 2017;13(4):381-387. doi:10.1016/j.jalz.2016.07.004
21. Sudom A, Talreja S, Danao J, et al. Molecular basis for the loss-of-function effects of the Alzheimer's disease-associated R47H variant of the immune receptor TREM2. *J Biol Chem*. Aug 10 2018;293(32):12634-12646. doi:10.1074/jbc.RA118.002352
22. McKenzie AT, Wang MH, Hauberg ME, et al. Brain Cell Type Specific Gene Expression and Co-expression Network Architectures. *Scientific Reports*. Jun 2018;88868. doi:10.1038/s41598-018-27293-5

23. Wang YM, Cella M, Mallinson K, et al. TREM2 Lipid Sensing Sustains the Microglial Response in an Alzheimer's Disease Model. *Cell*. Mar 2015;160(6):1061-1071. doi:10.1016/j.cell.2015.01.049
24. Poliani PL, Wang YM, Fontana E, et al. TREM2 sustains microglial expansion during aging and response to demyelination. *Journal of Clinical Investigation*. May 2015;125(5):2161-2170. doi:10.1172/jci77983
25. Nugent AA, Lin K, van Lengerich B, et al. TREM2 Regulates Microglial Cholesterol Metabolism upon Chronic Phagocytic Challenge. *Neuron*. Mar 2020;105(5):837-+. doi:10.1016/j.neuron.2019.12.007
26. Rueda-Carrasco J, Sokolova D, Lee SE, et al. Microglia-synapse engulfment via PtdSer-TREM2 ameliorates neuronal hyperactivity in Alzheimer's disease models. *Embo j*. Oct 4 2023;42(19):e113246. doi:10.15252/embj.2022113246
27. Cannon JP, O'Driscoll M, Litman GW. Specific lipid recognition is a general feature of CD300 and TREM molecules. *Immunogenetics*. Jan 2012;64(1):39-47. doi:10.1007/s00251-011-0562-4
28. Daws MR, Sullam PM, Niemi EC, Chen TT, Tchao NK, Seaman WE. Pattern recognition by TREM-2: Binding of anionic ligands. *Journal of Immunology*. Jul 2003;171(2):594-599.
29. Shirotani K, Hori Y, Yoshizaki R, et al. Aminophospholipids are signal-transducing TREM2 ligands on apoptotic cells. *Scientific Reports*. 2019/05/17 2019;9(1):7508. doi:10.1038/s41598-019-43535-6
30. Hsieh CL, Koike M, Spusta SC, et al. A role for TREM2 ligands in the phagocytosis of apoptotic neuronal cells by microglia. *Journal of Neurochemistry*. May 2009;109(4):1144-1156. doi:10.1111/j.1471-4159.2009.06042.x
31. Ibach M, Mathews M, Linnartz-Gerlach B, et al. A reporter cell system for the triggering receptor expressed on myeloid cells 2 reveals differential effects of disease-associated variants on receptor signaling and activation by antibodies against the stalk region. *Glia*. May 2021;69(5):1126-1139. doi:10.1002/glia.23953
32. Kober DL, Stuchell-Brereton MD, Kluender CE, et al. Functional insights from biophysical study of TREM2 interactions with apoE and A beta(1-42). Article; Early Access. *Alzheimers & Dementia*. 2020:14. doi:10.1002/alz.12194
33. Lessard CB, Malnik SL, Zhou YY, et al. High-affinity interactions and signal transduction between A beta oligomers and TREM2. *Embo Molecular Medicine*. Nov 2018;10(11)e9027. doi:10.15252/emmm.201809027
34. Zhao Y, Wu X, Li X, et al. TREM2 Is a Receptor for β-Amyloid that Mediates Microglial Function. *Neuron*. 2018;97(5):1023-1031.e7. doi:10.1016/j.neuron.2018.01.031
35. Zhong L, Wang Z, Wang D, et al. Amyloid-beta modulates microglial responses by binding to the triggering receptor expressed on myeloid cells 2 (TREM2). *Molecular Neurodegeneration*. 2018/03/27 2018;13(1):15. doi:10.1186/s13024-018-0247-7
36. Yeh FL, Wang Y, Tom I, Gonzalez LC, Sheng M. TREM2 Binds to Apolipoproteins, Including APOE and CLU/APOJ, and Thereby Facilitates Uptake of Amyloid-Beta by Microglia. *Neuron*. 2016;91(2):328-340. doi:https://doi.org/10.1016/j.neuron.2016.06.015
37. Oyanagi K, Kinoshita M, Suzuki-Kouyama E, et al. Adult onset leukoencephalopathy with axonal spheroids and pigmented glia (ALSP) and Nasu–Hakola disease: lesion staging and dynamic changes of axons and microglial subsets. https://doi.org/10.1111/bpa.12443. *Brain Pathology*. 2017/11/01 2017;27(6):748-769. doi:https://doi.org/10.1111/bpa.12443
38. Yuan P, Condello C, Keene CD, et al. TREM2 Haplodeficiency in Mice and Humans Impairs the Microglia Barrier Function Leading to Decreased Amyloid Compaction and Severe Axonal Dystrophy. *Neuron*. May 18 2016;90(4):724-39. doi:10.1016/j.neuron.2016.05.003
39. Piers TM, Cosker K, Mallach A, et al. A locked immunometabolic switch underlies TREM2 R47H loss of function in human iPSC-derived microglia. *Faseb Journal*. Feb 2020;34(2):2436-2450. doi:10.1096/fj.201902447R

40. Takahashi K, Rochford CDP, Neumann H. Clearance of apoptotic neurons without inflammation by microglial triggering receptor expressed on myeloid cells-2. *Journal of Experimental Medicine*. Feb 2005;201(4):647-657. doi:10.1084/jem.20041611
41. Garcia-Reitboeck P, Phillips A, Piers TM, et al. Human Induced Pluripotent Stem Cell-Derived Microglia-Like Cells Harboring TREM2 Missense Mutations Show Specific Deficits in Phagocytosis. *Cell Reports*. Aug 2018;24(9):2300-2311. doi:10.1016/j.celrep.2018.07.094
42. Xiang X, Werner G, Bohrmann B, et al. TREM2 deficiency reduces the efficacy of immunotherapeutic amyloid clearance. *EMBO Molecular Medicine*. 2016;8(9):992. doi:10.15252/emmm.201606370
43. Cantoni C, Bollman B, Licastro D, et al. TREM2 regulates microglial cell activation in response to demyelination in vivo. *Acta Neuropathologica*. Mar 2015;129(3):429-447. doi:10.1007/s00401-015-1388-1
44. Yokoi S, Suzuki K, Amano N, Yagishita S. FATTY-ACID ANALYSIS OF GALACTOLIPIDS AND GANGLIOSIDE IN THE BRAINS OF 4 CASES OF NASU-HAKOLA DISEASE. *Japanese Journal of Psychiatry and Neurology*. Dec 1989;43(4):695-701.
45. Ohtani Y, Miura S, Tamai Y, Kojima H, Kashima H. NEUTRAL LIPID AND SPHINGOLIPID COMPOSITION OF THE BRAIN OF A PATIENT WITH MEMBRANOUS LIPODYSTROPHY. *Journal of Neurology*. 1979;220(2):77-82. doi:10.1007/bf00313947
46. Yokoi S, Suzuki K, Amano N, Yagishita S. [Lipid chemical study of an autopsy case of Nasu-Hakola disease]. *No To Shinkei*. Feb 1988;40(2):141-7.
47. Phillips A, Villegas-Llerena C, Piers TM, Cosker K, Hardy J, Pocock JM. Loss of Function of TREM2 Results in Cytoskeletal Malfunction in Microglia. 2018:
48. Cella M, Buonsanti C, Strader C, Kondo T, Salmaggi A, Colonna M. Impaired differentiation of osteoclasts in TREM-2-deficient individuals. *Journal of Experimental Medicine*. Aug 2003;198(4):645-651. doi:10.1084/jem.20022220
49. Peng QS, Malhotra S, Torchia JA, Kerr WG, Coggeshall KM, Humphrey MB. TREM2-and DAP12-Dependent Activation of PI3K Requires DAP10 and Is Inhibited by SHIP1. *Science Signaling*. May 2010;3(122)ra38. doi:10.1126/scisignal.2000500
50. Jiang T, Tan L, Zhu X-C, et al. Upregulation of TREM2 Ameliorates Neuropathology and Rescues Spatial Cognitive Impairment in a Transgenic Mouse Model of Alzheimer's Disease. *Neuropsychopharmacology*. Dec 2014;39(13):2949-2962. doi:10.1038/npp.2014.164
51. Lee CYD, Daggett A, Gu XF, et al. Elevated TREM2 Gene Dosage Reprograms Microglia Responsivity and Ameliorates Pathological Phenotypes in Alzheimer's Disease Models. *Neuron*. Mar 2018;97(5):1032-+. doi:10.1016/j.neuron.2018.02.002
52. Song WM, Joshita S, Zhou Y, Ulland TK, Gilfillan S, Colonna M. Humanized TREM2 mice reveal microglia-intrinsic and -extrinsic effects of R47H polymorphism. *The Journal of Experimental Medicine*. 2018;doi:10.1084/jem.20171529
53. Wang S, Mustafa M, Yuede CM, et al. Anti-human TREM2 induces microglia proliferation and reduces pathology in an Alzheimer's disease model. *J Exp Med*. Sep 7 2020;217(9)doi:10.1084/jem.20200785
54. Ulrich JD, Finn MB, Wang Y, et al. Altered microglial response to A beta plaques in APPPS1-21 mice heterozygous for TREM2. *Molecular Neurodegeneration*. Jun 3 2014;920. doi:10.1186/1750-1326-9-20
55. Cheng-Hathaway PJ, Reed-Geaghan EG, Jay TR, et al. The Trem2 R47H variant confers loss-of-function-like phenotypes in Alzheimer's disease. *Molecular Neurodegeneration*. 2018/06/01 2018;13(1):29. doi:10.1186/s13024-018-0262-8
56. Ulland TK, Song WM, Huang SCC, et al. TREM2 Maintains Microglial Metabolic Fitness in Alzheimer's Disease. *Cell*. Aug 2017;170(4):649-+. doi:10.1016/j.cell.2017.07.023
57. Parhizkar S, Arzberger T, Brendel M, et al. Loss of TREM2 function increases amyloid seeding but reduces plaque-associated ApoE. *Nature Neuroscience*. 2019/02/01 2019;22(2):191-204. doi:10.1038/s41593-018-0296-9

58. Yuan P, Condello C, Keene CD, et al. TREM2 Haplodeficiency in Mice and Humans Impairs the Microglia Barrier Function Leading to Decreased Amyloid Compaction and Severe Axonal Dystrophy. *Neuron*. May 2016;90(4):724-739. doi:10.1016/j.neuron.2016.05.003
59. Kiskis J, Fink H, Nyberg L, Thyr J, Li J-Y, Enejder A. Plaque-associated lipids in Alzheimer's diseased brain tissue visualized by nonlinear microscopy. *Scientific reports*. 2015;5:13489-13489. doi:10.1038/srep13489
60. Touboul D, Gaudin M. Lipidomics of Alzheimer's disease. *Bioanalysis*. Feb 2014;6(4):541-61. doi:10.4155/bio.13.346
61. Kaya I, Zetterberg H, Blennow K, Hanrieder J. Shedding Light on the Molecular Pathology of Amyloid Plaques in Transgenic Alzheimer's Disease Mice Using Multimodal MALDI Imaging Mass Spectrometry. *ACS Chem Neurosci*. Jul 18 2018;9(7):1802-1817. doi:10.1021/acschemneuro.8b00121
62. Kim M, Nevado-Holgado A, Whiley L, et al. Association between Plasma Ceramides and Phosphatidylcholines and Hippocampal Brain Volume in Late Onset Alzheimer's Disease. *J Alzheimers Dis*. 2017;60(3):809-817. doi:10.3233/JAD-160645
63. Alafuzoff I, Arzberger T, Al-Sarraj S, et al. Staging of neurofibrillary pathology in Alzheimer's disease: A study of the BrainNet Europe consortium. *Brain Pathology*. 2008;18(4):484-496. NOT IN FILE.
64. Braak H, Braak E. Neuropathological Staging of Alzheimer-Related Changes. *Acta Neuropathologica*. 1991;82(4):239-259. NOT IN FILE.
65. Alafuzoff I, Pikkarainen M, Al-Sarraj S, et al. Interlaboratory comparison of assessments of Alzheimer disease-related lesions: a study of the BrainNet Europe consortium. *Journal of Neuropathology and Experimental Neurology*. Aug 2006;65(8):740-757.
66. Josephs KA, Murray ME, Whitwell JL, et al. Staging TDP-43 pathology in Alzheimer's disease. *Acta Neuropathologica*. Mar 2014;127(3):441-450. doi:10.1007/s00401-013-1211-9
67. Braak H, Del Tredici K, Rub U, de Vos RAI, Steur E, Braak E. Staging of brain pathology related to sporadic Parkinson's disease. *Neurobiol Aging*. Mar-Apr 2003;24(2):197-211. Pii s0197-4580(02)00065-9. doi:10.1016/s0197-4580(02)00065-9
68. Ebshiana AA, Snowden SG, Thambisetty M, Parsons R, Hye A, Legido-Quigley C. Metabolomic method: UPLC-q-ToF polar and non-polar metabolites in the healthy rat cerebellum using an in-vial dual extraction. *PLoS One*. 2015;10(4):e0122883. doi:10.1371/journal.pone.0122883
69. Varma VR, Wang Y, An Y, et al. Bile acid synthesis, modulation, and dementia: A metabolomic, transcriptomic, and pharmacoepidemiologic study. *PLOS Medicine*. 2021;18(5):e1003615. doi:10.1371/journal.pmed.1003615
70. J P, D B, S D, D S. nlme: Linear and Nonlinear Mixed Effects Models. R package version 3.1-152. 2021. https://CRAN.R-project.org/package=nlme.
71. Langfelder P, Luo R, Oldham MC, Horvath S. Is my network module preserved and reproducible? *PLoS Comput Biol*. Jan 20 2011;7(1):e1001057. doi:10.1371/journal.pcbi.1001057
72. Lee BC, Khelashvili G, Falzone M, Menon AK, Weinstein H, Accardi A. Gating mechanism of the extracellular entry to the lipid pathway in a TMEM16 scramblase. *Nat Commun*. Aug 14 2018;9(1):3251. doi:10.1038/s41467-018-05724-1
73. Neher JJ, Emmrich JV, Fricker M, Mander PK, Thery C, Brown GC. Phagocytosis executes delayed neuronal death after focal brain ischemia. *Proceedings of the National Academy of Sciences of the United States of America*. Oct 22 2013;110(43):E4098-E4107. doi:10.1073/pnas.1308679110
74. Brown GC, Neher JJ. Microglial phagocytosis of live neurons. *Nature Reviews Neuroscience*. Apr 2014;15(4):209-216. doi:10.1038/nrn3710
75. Harayama T, Riezman H. Understanding the diversity of membrane lipid composition. *Nature Reviews Molecular Cell Biology*. 2018/05/01 2018;19(5):281-296. doi:10.1038/nrm.2017.138
76. Lee-Gosselin A, Jury-Garfe N, You Y, et al. TREM2-Deficient Microglia Attenuate Tau Spreading In Vivo. *Cells*. Jun 10 2023;12(12)doi:10.3390/cells12121597

77. Brelstaff JH, Mason M, Katsinelos T, et al. Microglia become hypofunctional and release metalloproteases and tau seeds when phagocytosing live neurons with P301S tau aggregates. *Sci Adv*. Oct 22 2021;7(43):eabg4980. doi:10.1126/sciadv.abg4980
78. Asai H, Ikezu S, Tsunoda S, et al. Depletion of microglia and inhibition of exosome synthesis halt tau propagation. *Nature Neuroscience*. 2015/11/01 2015;18(11):1584-1593. doi:10.1038/nn.4132
79. Chung H, Brazil MI, Soe TT, Maxfield FR. Uptake, degradation, and release of fibrillar and soluble forms of Alzheimer's amyloid beta-peptide by microglial cells. *J Biol Chem*. Nov 5 1999;274(45):32301-8. doi:10.1074/jbc.274.45.32301
80. Damisah EC, Hill RA, Rai A, et al. Astrocytes and microglia play orchestrated roles and respect phagocytic territories during neuronal corpse removal in vivo. *Sci Adv*. Jun 2020;6(26):eaba3239. doi:10.1126/sciadv.aba3239
81. Augustinack JC, Schneider A, Mandelkow E-M, Hyman BT. Specific tau phosphorylation sites correlate with severity of neuronal cytopathology in Alzheimer's disease. *Acta Neuropathologica*. 2002/01/01 2002;103(1):26-35. doi:10.1007/s004010100423
82. Kleinberger G, Yamanishi Y, Suarez-Calvet M, et al. TREM2 mutations implicated in neurodegeneration impair cell surface transport and phagocytosis. *Science Translational Medicine*. Jul 2014;6(243)243ra86. doi:10.1126/scitranslmed.3009093
83. Neumann H, Kotter M, Franklin R. Debris clearance by microglia: an essential link between degeneration and regeneration. *Brain*. 2009;132:288 - 295.
84. Sierra A, Beccari S, Diaz-Aparicio I, Encinas JM, Comeau S, Tremblay M. Surveillance, phagocytosis, and inflammation: how never-resting microglia influence adult hippocampal neurogenesis. *Neural Plast*. 2014;2014:610343. doi:10.1155/2014/610343
85. Sierra A, Encinas JM, Deudero JJ, et al. Microglia shape adult hippocampal neurogenesis through apoptosis-coupled phagocytosis. *Cell Stem Cell*. Oct 8 2010;7(4):483-95. doi:10.1016/j.stem.2010.08.014
86. Kono H, Rock KL. How dying cells alert the immune system to danger. *Nat Rev Immunol*. Apr 2008;8(4):279-89. doi:10.1038/nri2215
87. Consortium. SEA-AD. Study data were generated from postmortem brain tissue obtained from the University of Washington BioRepository and Integrated Neuropathology (BRaIN) laboratory and Precision Neuropathology Core, which is supported by the NIH grants for the UW Alzheimer's Disease Research Center (NIA grants: P50AG005136 and P30AG066509) and the Adult Changes in Thought Study (NIA grants: U01AG006781 and U19AG066567).
88. Kim HY, Huang BX, Spector AA. Phosphatidylserine in the brain: metabolism and function. *Prog Lipid Res*. Oct 2014;56:1-18. doi:10.1016/j.plipres.2014.06.002
89. Montani L. Lipids in regulating oligodendrocyte structure and function. *Seminars in Cell & Developmental Biology*. 2021/04/01/ 2021;112:114-122. doi:https://doi.org/10.1016/j.semcdb.2020.07.016
90. Fitzner D, Bader JM, Penkert H, et al. Cell-Type- and Brain-Region-Resolved Mouse Brain Lipidome. *Cell Reports*. 2020;32(11)doi:10.1016/j.celrep.2020.108132
91. Carbajosa G, Malki K, Lawless N, et al. TREM2 impacts brain microglia, oligodendrocytes and endothelial co-expression modules revealing genes and pathways important in Alzheimer's disease. *Biorxv*. 2021 2021;
92. Schmitt S, Castelvetri LC, Simons M. Metabolism and functions of lipids in myelin. *Biochim Biophys Acta*. Aug 2015;1851(8):999-1005. doi:10.1016/j.bbalip.2014.12.016
93. Cutler RG, Kelly J, Storie K, et al. Involvement of oxidative stress-induced abnormalities in ceramide and cholesterol metabolism in brain aging and Alzheimer's disease. *Proc Natl Acad Sci U S A*. Feb 17 2004;101(7):2070-5. doi:10.1073/pnas.0305799101
94. Alessenko AV, Albi E. Exploring Sphingolipid Implications in Neurodegeneration. *Front Neurol*. 2020;11:437. doi:10.3389/fneur.2020.00437

95. Kihara A. Synthesis and degradation pathways, functions, and pathology of ceramides and epidermal acylceramides. *Progress in Lipid Research*. 2016/07/01/ 2016;63:50-69. doi:https://doi.org/10.1016/j.plipres.2016.04.001
96. McGrath ER, Himali JJ, Xanthakis V, et al. Circulating ceramide ratios and risk of vascular brain aging and dementia. *Ann Clin Transl Neurol*. Feb 2020;7(2):160-168. doi:10.1002/acn3.50973
97. Baloni P, Arnold M, Buitrago L, et al. Multi-Omic analyses characterize the ceramide/sphingomyelin pathway as a therapeutic target in Alzheimer's disease. *Commun Biol*. Oct 8 2022;5(1):1074. doi:10.1038/s42003-022-04011-6
98. Toledo JB, Arnold M, Kastenmuller G, et al. Metabolic network failures in Alzheimer's disease: A biochemical road map. *Alzheimers Dement*. Sep 2017;13(9):965-984. doi:10.1016/j.jalz.2017.01.020
99. Varma VR, Oommen AM, Varma S, et al. Brain and blood metabolite signatures of pathology and progression in Alzheimer disease: A targeted metabolomics study. *Plos Medicine*. Jan 2018;15(1)e1002482. doi:10.1371/journal.pmed.1002482
100. Chan RB, Oliveira TG, Cortes EP, et al. Comparative lipidomic analysis of mouse and human brain with Alzheimer disease. *J Biol Chem*. Jan 20 2012;287(4):2678-88. doi:10.1074/jbc.M111.274142
101. Dehghan A, Pinto RC, Karaman I, et al. Metabolome-wide association study on ABCA7 indicates a role of ceramide metabolism in Alzheimer's disease. *Proc Natl Acad Sci U S A*. Oct 25 2022;119(43):e2206083119. doi:10.1073/pnas.2206083119
102. Wretlind A, Curovic VR, Suvitaival T, et al. Ceramides as Risk Markers for Future Cardiovascular Events and All-Cause Mortality in Long-standing Type 1 Diabetes. *Diabetes*. Oct 1 2023;72(10):1493-1501. doi:10.2337/db23-0052
103. Boudesco C, Nonneman A, Cinti A, et al. Novel potent liposome agonists of triggering receptor expressed on myeloid cells 2 phenocopy antibody treatment in cells. *Glia*. Dec 2022;70(12):2290-2308. doi:10.1002/glia.24252
104. Filipello F, You SF, Mirfakhar FS, et al. Defects in lysosomal function and lipid metabolism in human microglia harboring a TREM2 loss of function mutation. *Acta Neuropathol*. Jun 2023;145(6):749-772. doi:10.1007/s00401-023-02568-y
105. Prakash P, Manchanda P, Paouri E, et al. Amyloid beta Induces Lipid Droplet-Mediated Microglial Dysfunction in Alzheimer's Disease. *bioRxiv*. Jun 6 2023;doi:10.1101/2023.06.04.543525
106. Haney MS, Palovics R, Munson CN, et al. APOE4/4 is linked to damaging lipid droplets in Alzheimer's disease microglia. *Nature*. Apr 2024;628(8006):154-161. doi:10.1038/s41586-024-07185-7
107. Sanderson JM. The association of lipids with amyloid fibrils. *J Biol Chem*. Aug 2022;298(8):102108. doi:10.1016/j.jbc.2022.102108
108. Czubowicz K, Jęśko H, Wencel P, Lukiw WJ, Strosznajder RP. The Role of Ceramide and Sphingosine-1-Phosphate in Alzheimer's Disease and Other Neurodegenerative Disorders. *Mol Neurobiol*. Aug 2019;56(8):5436-5455. doi:10.1007/s12035-018-1448-3
109. Liu Q, Zhang J. Lipid metabolism in Alzheimer's disease. *Neurosci Bull*. Apr 2014;30(2):331-45. doi:10.1007/s12264-013-1410-3
110. Cutler RG, Kelly J, Storie K, et al. Involvement of oxidative stress-induced abnormalities in ceramide and cholesterol metabolism in brain aging and Alzheimer's disease. *Proceedings of the National Academy of Sciences of the United States of America*. Feb 2004;101(7):2070-2075. doi:10.1073/pnas.0305799101
111. Zeng C, Lee JT, Chen H, Chen S, Hsu CY, Xu J. Amyloid-beta peptide enhances tumor necrosis factor-alpha-induced iNOS through neutral sphingomyelinase/ceramide pathway in oligodendrocytes. *J Neurochem*. Aug 2005;94(3):703-12. doi:10.1111/j.1471-4159.2005.03217.x
112. Grimm MO, Grimm HS, Pätzold AJ, et al. Regulation of cholesterol and sphingomyelin metabolism by amyloid-beta and presenilin. *Nat Cell Biol*. Nov 2005;7(11):1118-23. doi:10.1038/ncb1313

113. Tanabe F, Nakajima T, Ito M. The thiol proteinase inhibitor E-64-d ameliorates amyloid-β-induced reduction of sAPPα secretion by reversing ceramide-induced protein kinase C down-regulation in SH-SY5Y neuroblastoma cells. *Biochem Biophys Res Commun*. Nov 8 2013;441(1):256-61. doi:10.1016/j.bbrc.2013.10.045
114. Prakash P, Manchanda P, Paouri E, et al. Amyloid β Induces Lipid Droplet-Mediated Microglial Dysfunction in Alzheimer's Disease. *bioRxiv*. Jun 6 2023;doi:10.1101/2023.06.04.543525
115. Wei W, Zhang L, Xin W, et al. TREM2 regulates microglial lipid droplet formation and represses post-ischemic brain injury. *Biomedicine & Pharmacotherapy*. 2024/01/01/ 2024;170:115962. doi:https://doi.org/10.1016/j.biopha.2023.115962
116. Gouna G, Klose C, Bosch-Queralt M, et al. TREM2-dependent lipid droplet biogenesis in phagocytes is required for remyelination. *J Exp Med*. Oct 4 2021;218(10)doi:10.1084/jem.20210227
117. Nugent AA, Lin K, van Lengerich B, et al. TREM2 Regulates Microglial Cholesterol Metabolism upon Chronic Phagocytic Challenge. *Neuron*. 2020;105(5):837-854.e9. doi:10.1016/j.neuron.2019.12.007
118. Zhang X, Tian Q, Liu D, et al. Causal association of circulating cholesterol levels with dementia: a mendelian randomization meta-analysis. *Translational Psychiatry*. 2020/05/12 2020;10(1):145. doi:10.1038/s41398-020-0822-x
119. Sáiz-Vazquez O, Puente-Martínez A, Ubillos-Landa S, Pacheco-Bonrostro J, Santabárbara J. Cholesterol and Alzheimer's Disease Risk: A Meta-Meta-Analysis. *Brain Sci*. Jun 18 2020;10(6)doi:10.3390/brainsci10060386
120. Tan JS, Hu MJ, Yang YM, Yang YJ. Genetic Predisposition to Low-Density Lipoprotein Cholesterol May Increase Risks of Both Individual and Familial Alzheimer's Disease. *Front Med (Lausanne)*. 2021;8:798334. doi:10.3389/fmed.2021.798334
121. Liu Y, Thalamuthu A, Mather KA, et al. Plasma lipidome is dysregulated in Alzheimer's disease and is associated with disease risk genes. *Transl Psychiatry*. Jun 7 2021;11(1):344. doi:10.1038/s41398-021-01362-2
122. Oresic M, Hyotylainen T, Herukka SK, et al. Metabolome in progression to Alzheimer's disease. *Transl Psychiatry*. Dec 13 2011;1(12):e57. doi:10.1038/tp.2011.55
123. Whiley L, Sen A, Heaton J, et al. Evidence of altered phosphatidylcholine metabolism in Alzheimer's disease. *Neurobiol Aging*. Feb 2014;35(2):271-8. doi:10.1016/j.neurobiolaging.2013.08.001
124. Arnold M, Nho K, Kueider-Paisley A, et al. Sex and APOE epsilon4 genotype modify the Alzheimer's disease serum metabolome. *Nat Commun*. Mar 2 2020;11(1):1148. doi:10.1038/s41467-020-14959-w
125. Novotny BC, Fernandez MV, Wang C, et al. Metabolomic and lipidomic signatures in autosomal dominant and late-onset Alzheimer's disease brains. *Alzheimers Dement*. May 2023;19(5):1785-1799. doi:10.1002/alz.12800

Supplementary material

Supplementary material is available online.

Figure Legends

Figure 1. Diagramatic study flow.

Figure 2. Associations of lipid modules with post-mortem diagnosis and TREM2 status. a) Heatmaps showing the relationships of BA9 and Hippocampus (HC) modules with 1) Post-mortem AD diagnosis (i.e. AD/TREM2^{var} and AD/TREM2^{WT} combined vs Control/TREM2^{WT} donors), 2) AD/TREM2^{WT} brain donors vs Control/TREM2^{WT} donors, 3) AD/TREM2^{var} vs Control/TREM2^{WT} donors, 4) TREM2^{var} vs TREM2^{WT} in AD donors, and 4) Number of APOEε4 alleles. The number of lipids in each module is shown underneath each module name.

*p<0.05, **p<0.00125. The colour of the tiles reflects the strength of the association (beta) with blue tiles indicating a decrease and red tiles indicating an increase in lipid levels in AD donors vs controls, in TREM2+ vs TREM2- carriers and in donors with a higher number of APOEε4 alleles. CTL=controls, AD=Alzheimer's Disease, APOE4=number of APOEε4 alleles. *The BA9 blue module corresponds to the Hippocampus brown module; the BA9 brown module corresponds to the Hippocampus turquoise module; the BA9 turquoise module corresponds to the Hippocampus blue module; the BA9 yellow module corresponds to the Hippocampus yellow and turquoise modules.*

Figure 3. Association of hub lipids with Post-mortem AD diagnosis and with TREM2 status. 1) Post-mortem AD diagnosis (i.e. AD/TREM2^{var} and AD/TREM2^{WT} combined vs Control/TREM2^{WT} donors), 2) AD/TREM2^{WT} vs Control/TREM2^{WT} donors, 3) AD/TREM2^{var} vs Control/TREM2^{WT} donors, 4) TREM2^{var} vs TREM2^{WT} AD donors, (BA9 and Hippocampus combined) using generalised least squares and adjusting for sex, age (at death), post-mortem delay and APOE4 genotype. The columns on the right of the plot indicate the lipid family and module each lipid is assigned to, in each brain region. Lipid levels are standardised to a mean of 0 and SD of 1. Bonferroni adjusted threshold p<0.00146.

CTL=control donors; AD=Alzheimer's disease donors; CER=Ceramide; SM=Sphingomyelin; PA=Phosphatidic acid, PC=Phosphatidyl-choline, PI=Phosphatidyl-inositol; PS=Phosphatidyl-serine; PE=Phosphatidyl-ethanolamine.

Figure 4. Levels of Cer(d38:1) and PS(32:1) in AD and Controls, and in TREM2^{WT} and TREM2^{var} carriers in BA9 and the Hippocampus. Cer(d38:1) was the top turquoise module lipid associated with AD (combined AD/TREM2^{var} and AD/TREM2^{WT}) vs Control/TREM2^{WT} donors and with AD/TREM2^{var} vs Control/TREM2^{WT} donors, and

PS(32:1) was the top "hub" lipid in the turquoise module (i.e. the hub lipid more closely associated to its module).

Table 1. Cohort Characteristics.

	BA9 (n=55)			EC (n=47)		
Diagnosis, n	AD (n=34)	Control (n=21)	P*	AD (n=27)	Control (n=20)	P*
Females/Males[% Female]	20/34[59%]	8/21[38.1%]	0.224	16/27[59%]	8/20[40%]	0.312
Age (years), mean (sd)	74.4 (12.8)	72.4 (12.6)	0.566	76.5 (11.9)	72.7 (12.9)	0.300
APOE ε4 alleles, n (0/1/2)	6/21/7	17/3/1	2.25e-05	4/18/5	16/3/1	4.58e-05
PMD (hrs), mean (sd)	32.56 (22.5)	32.81 (18.1)	0.965	32.41 (21.66)	32.4 (19.30)	0.999
$TREM2^{var}$/total samples, n[% $TREM2^{var}$]	14/34[28%]	0/21[0%]	2.0e-03	7/27[16%]	0/20[0%]	0.040
$TREM2^{var}$breakdown p.R47H/p.T96K/p.D87N /p.D39E/p.Q33X/p.G58A	7/1/3/1/1/1	0/0/0/0/0/0	NA	4/1/1/0/1/0	0/0/0/0/0/0	NA

*P-values based on one-way analysis of variance for continuous variables or Chi square test for categorical variables

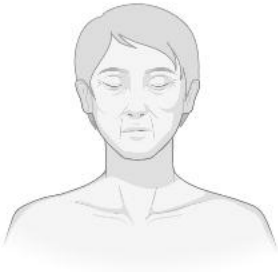

55 donors

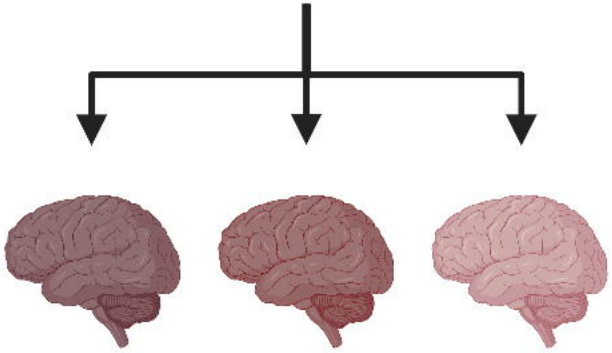

AD + TREM2^{var}

AD + TREM2^{wt}

Healthy Control

Tissue From Two Regions

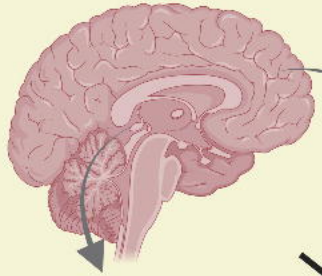

BA9 Preassociated Cortex

Hippocampus

Lipid Extraction

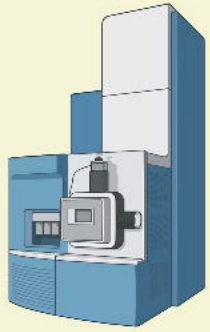

Mass Spectrometry

Lipid networks with WGCNA

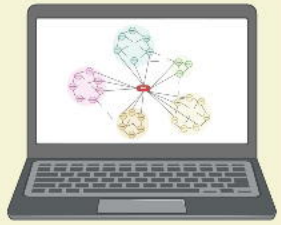

Data Analysis

One Module Associated with AD and/or TREM2^{var}

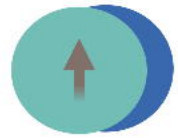

BA9 Turquise
Hippocampus Blue

Lipids in these modules were increased in both AD donors and TREM2^{var} carriers (additive effect)

Lipids: Cer, PS and SM

Cer (d38:1)

Strongest AD/TREM2^{var} associated lipid

PS (32:1)

Leading "hub" lipid